

Research Article

Muryadin*, Teguh Muttaqie, Cahyo Sasmito, Fariz Maulana Noor, Andi C. P. T. Nugroho, Dany Hendrik Priatno, Buddin Al Hakim, Abid Paripurna Fuadi, Muh Hisyam Khoirudin, Teguh Wibowo, and Arfis Maydino F. Putra

Dynamic response of high-speed craft bottom panels subjected to slamming loadings

<https://doi.org/10.1515/cls-2022-0190>

received August 02, 2022; accepted February 25, 2023

Abstract: The inelastic deformation of a 30 m high-speed craft (HSC) subjected to slamming pressure is the main topic of this research. In this work, the commercial software package ABAQUS FEA is used to predict the structural behavior, especially in the hull area under the chine. Dynamic explicit solver simulations are done to predict plastic deformation. Before the principal analysis of the actual size of the ship hull structure model, the numerical studies were validated against relevant experimental data from the previous open literature. A reassessment of the design guidelines was also done to forecast the slamming load on the HSC structure. Then, with the slamming load pressure increased to the design limit, a parametric analysis was also conducted with two different idealizations of the pressure type: rectangular and triangular. Finally, this study identifies the variables that must be considered when calculating the degree of structural deformation brought on by slamming loads.

Keywords: slamming, dynamic pressure, nonlinear FE analysis, plastic deformation

1 Introduction

Fast patrol boats are built to travel at high speed. As a result, the bottom panels of the ship will experience impact loads which can result in significant plastic deformation when the ship is traveling at relatively high speeds in irregular waves. The impact of water on ship hulls is referred to as slamming. These slamming loads can be quite intense in extreme sea conditions, with a characteristic of peak pressure up to 5,000 kPa with a short duration [1].

Today's high-speed craft designers rely heavily on semi-empirical design methodologies based on classification societies' design standards [2,3]. These methods have the advantage of being simple, robust, and straightforward, but this can come at the expense of accuracy and makes it difficult to show the actual response of the ship's structure under such loading. This challenge in high-speed craft (HSC) design poses limitations on designing a bottom substructure that is reliable against slamming and can reach the target speed. A strong structure will have a significant weight compensation in the conventional design formula. An alternative approach is direct calculations which imply loads and structure load carrying capacity and have been proven necessary in the design of the Visby Class Corvette, where the entire structure is made of carbon composite sandwich to achieve the lightest structure [4]. Many detailed experimental and numerical studies consider this short period of pressure loading arise [5–9]. This study stated that inelastic deformation strongly depends on the impact duration and the plate aspect ratio. In addition, the shape of the pressure profile used and the magnitude of the peak pressure also affect the structure's response to the slamming load. In some of these studies, constitutive material and reduction due to the influence of heat-affected zones (HAZ) are also taken into account in the analysis. The application of aluminum material is indeed widely used in several types of HSC. The value of HAZ on aluminum is explained

* **Corresponding author: Muryadin**, Research Center for Hydrodynamics Technology, National Research and Innovation Agency, BRIN, Surabaya 60112, Indonesia, e-mail: mury001@brin.go.id, tel: +62 (31) 5953195

Teguh Muttaqie, Cahyo Sasmito, Fariz Maulana Noor, Andi C. P. T. Nugroho, Dany Hendrik Priatno, Buddin Al Hakim, Abid Paripurna Fuadi, Muh Hisyam Khoirudin: Research Center for Hydrodynamics Technology, National Research and Innovation Agency, BRIN, Surabaya 60112, Indonesia

Teguh Wibowo: Directorate of Fleet Monitoring and Operation, Directorate General of Marine and Fisheries Resources Surveillance, Ministry of Marine Affairs and Fisheries Republic of Indonesia, Jakarta 10110, Indonesia

Arfis Maydino F. Putra: Department of Naval Architecture and Ocean Engineering, Marine Hydro-Science and Engineering Laboratory, Osaka University, Osaka 5650871, Japan

which states that the magnitude of the effect of HAZ in reducing the elastic limit of the material is 0.67 [10].

The slamming load repeatedly occurs under certain conditions, resulting in a different impact response in a single impact loading. Mori [11] has previously investigated the effects of repeated impact loading on slamming loads. Recently, these findings were analyzed numerically and shared the same phenomenon [12]. According to the investigations, the impulsive pressure at the time of the first incident strongly influences the permanent set deformation. It is possible for the slamming load to repeatedly occur, in which case the permanent set will remain constant regardless of the impulse or aspect ratio. This response has been described previously that the damage to the clamped aluminum plate due to impulse loading, in several failure modes, one of which is a large inelastic deformation accompanied by tensile tears along the clamping boundary [13].

This present article investigates the structural response of stiffened bottom panels as a representative of high-speed craft, as shown in Figure 1. The lower portion of the forward hull structure may abruptly make contact with water when the bow has a high flare. Figure 2 depicts the slamming events observed in the HSC model at the BRIN hydrodynamics laboratory.

The article is organized as follows. The representative slamming test data gathered from the published test reports used for the validations are presented in Section 2 of the report. Section 3 outlines the detailed nonlinear finite element analysis (FEA) for the 30 m high-speed craft. Materials AL5083-H116 and AL6061-T6 [14] are used to construct the hull of this ship. In this section, there is also information regarding criteria related to design due to slamming. All of the simulations are done with ABAQUS FEA [15]. Overall, Section 4 highlights certain parameters that should be considered

when calculating the degree of structural deformation caused by slamming loads.

2 Slamming test data

As the speed of the ship rises, the bottom panel at the forebody of the high-speed craft is more likely to sustain slamming loads. The value of the slamming load is affected by the influence of momentum when the ship cruises and the weight of the boat itself in this occurrence. The slamming load is distributed along the bottom panel. In the simulation, the load is applied and distributed equally throughout the plate. In this dynamic load profile, the peak stress is relatively high in a short period. An impulsive loading is defined as a substantial amount of dynamic stress applied in a short period. This pressure value can fluctuate between 100 and 200 kPa in a matter of 0.02–0.03 seconds.

All simulations assumed the load was evenly distributed throughout the entire plate surface. As shown in Figure 3, the idealized dynamic pressure loading is presented in two ways: an idealized rectangular pressure and a triangle pulse with linear decay. This load profile idealizes the actual slamming load from the real test pressure as described in Figure 3(a). This pressure profile is taken from experiments conducted by Mori (1977) [11]. The P_0 value is the maximum peak pressure during slamming, and τ is the pressure duration. Figure 3(b) shows the time history for the idealized rectangular pressure profile [7]. Figure 3(c) shows the triangular-type pressure profile idealizes Langdon's impulsive loading experiment [13]. Based on the two profiles, the actual duration of the peak impulse induced by the slamming appears to be higher than the basic period of the impacted plate. As a



Figure 1: Photograph of Class 'C' patrol boat owned by the Marine Affairs and Fisheries Ministry Republic of Indonesia.

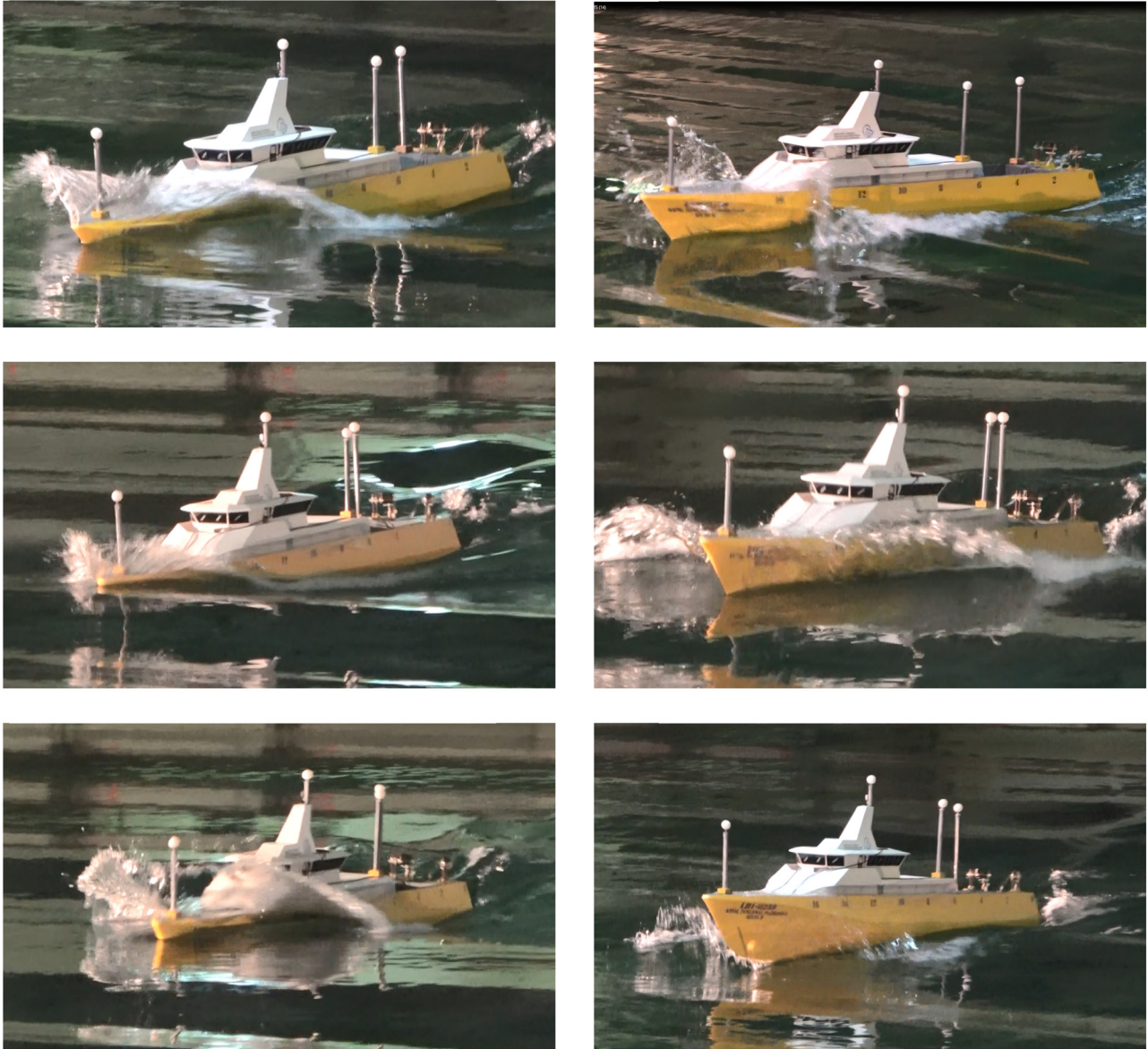


Figure 2: Slamming of high-speed craft model during seakeeping test.

result, it is concluded in this idealization that the effect of the tail on the level of damage can be ignored.

2.1 Benchmark test model

In this section, we describe a numerical prediction method validated using several studies found in the open literature. According to the literature review findings, studies of impulsive loading and slamming tests are very limited. This validation study has two types of models: rigid plates and unstiffened plates. Figure 4 shows the benchmark model used as a reference in this study. The details can be found in the literature [5,11,13]. Aluminum alloys

such as AL5083-H116 and AL5083-O were used in this simulation.

The first model is a stiffener plate measuring $2,400 \text{ mm} \times 1,800 \text{ mm}$ with a thickness of 1 mm equipped with three horizontal bar stiffeners measuring $\text{FB } 160 \times 8$ at equal distances. This model is a simplification of the bottom panel of the 80 m HSC structure. In this model, the HAZ is applied as a yield reduction due to the welding process on aluminum. This value is approximately 30% of the intact material (AL5083-H116). Using a mesh convergence study, this area was modeled at 20 mm according to predefined mesh size. The dynamic pressure load uses rectangular pressure idealization. The calculating time is longer than the time required for dynamic pressure loading. The calculation

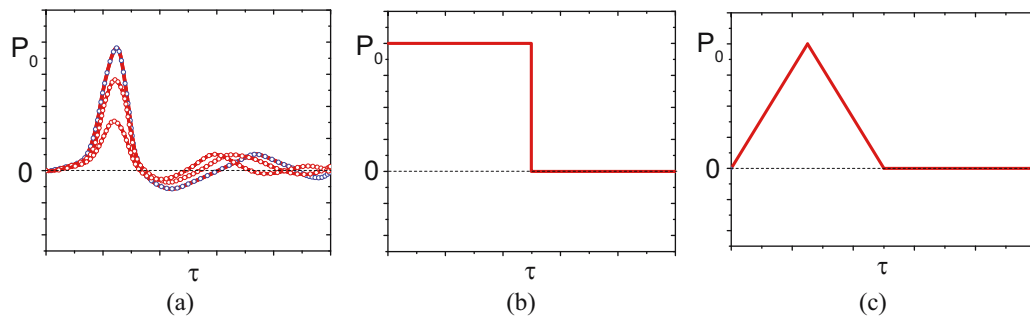


Figure 3: Pressure histories for slamming simulation: (a) experimental pressure, (b) idealized rectangular pressure, and (c) idealized triangle pressure.

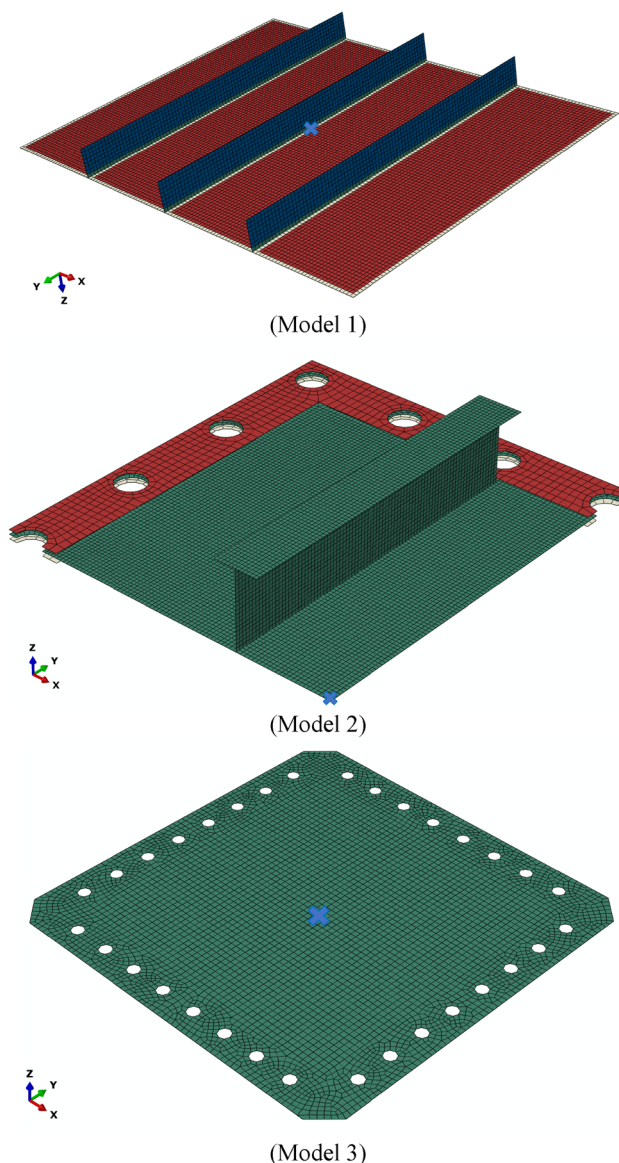


Figure 4: Benchmark test model for FEM validation.

time is set to 50 ms, which allows residual vibrations to be captured.

The second model uses the AL5083-O rigid plate model with a size of 1,000 mm \times 900 mm and a thickness of 6 mm. This model is reinforced using T stiffeners 94 \times 56 \times 6 with a distance of 246 mm. The model is clamped using a 72 mm wide plate where the four edges of this plate are fully restrained. The FE mesh size model used is 5 mm. This study uses a quarter-symmetric model to save computational time. The width of HAZ was set to be five times of element mesh. The detailed material for each model is reported in the original references. These three model simulations were validated based on the strategies described in Table 1. Structural damping was not included in the simulations because it was found to have a slight influence on plastic deformation [7].

The third model is a 660 mm \times 660 mm plate fixed on all four sides using a clamp plate and 22 mm bolt. Thus, the clamping model limits translational and rotational moving. Therefore, the boundary condition is fully clamped. The idealized load is set to 100 ms, and the peak pressure is varied up to 200 kPa in a triangular-type pressure pulse. The plates are made from two different aluminum alloy materials, namely, AL1 and AL2. The uniaxial tensile tests were performed from test pieces cut from the plate material in two longitudinal and transverse directions. In the numerical simulation, a simplification has been taken using the average value measured from the two directions.

2.2 Material

The influence of the HAZ must be incorporated into material modeling. As a result of the welding process, the favorable heat treatment acquired from the initial

Table 1: Numerical strategies of the benchmark test model

FE Set up	Model 1	Model 2	Model 3
Plate size	2,400 mm × 1,800 mm	1,000 mm × 900 mm	660 mm × 660 mm
Thickness	$t = 11$ mm	$t = 6$ mm	$t = 1$ mm
Stiffener size	FB. 160 mm × 8 mm	T. 94 mm × 56 mm × 6 mm	N/A
FE idealization	Full size	Quarter size	Full size
Converged mesh size	20 mm	5 mm	10 mm
Element type	S4R	S4R	S4R
Pressure type	Rectangular	Triangular	Triangular
BC type	Clamped at 4 sides	Clamped and symmetric BC	Clamped and symmetric BC
HAZ applied	Yes	Yes	N/A
Material definition	Aluminum true stress–strain	Aluminum true stress–strain	Aluminum true stress–strain
Analysis step	Dynamic explicit	Dynamic explicit	Dynamic explicit

material can be removed. It should be noted that the material's elastic limit is reduced due to welding processes. Figure 5 shows the relation in terms of the true stress–strain of the 5083-H116 aluminum alloy HAZ and base material used for model 1 in the FE analysis. The actual stress and strain are converted from the engineering stress and the engineering strain as described as follows:

$$\sigma_t = \sigma_e(\varepsilon_e + 1), \quad (1)$$

$$\varepsilon_t = \ln(\varepsilon_e + 1). \quad (2)$$

2.3 Numerical validation

In this section, the numerical validation with the benchmark test model was presented in a total of six numerical validation studies from three different models. After the elastic spring-back, the final plastic deformation has taken

at the average value. The detailed permanent plastic deformation with the described load-pulse parameters is shown in Table 2. The maximum deformation occurs at the model center as it oscillates with time as shown with a blue cross marked in Figure 4. The permanent set from the numerical and the benchmark model were in good agreement. Only for the last model, ALD052-2, the permanent set from the experiment was more significant than predicted. This could be due to the idealized load and boundary conditions, which may not be similar to the actual test conditions.

Figures 6 and 7 show a representative time history of the slamming response on a simplified substructure (model 1) measured from a single point node. This lateral displacement is measured at the center of the plate, which is the weld line of the second stiffener. The relationship between the pressure magnitude and the permanent set is clearly described. It is noted that the square-type pressure loading is used in this analysis. The pressure pulse duration is 20 ms, whereas the numerical time is set to 50 ms. The unloading process is barely visible at a pressure of 200 kPa.

On the other hand, at 400 kPa, a large plastic deformation gap is seen during the unloading process. The maximum deformation reaches a value of 80 mm until a permanent set after the spring-back occurs at 58 mm. This process can occur when high-speed craft launches off waves and impacts shallow water levels during bad weather conditions.

The simulation can explain the behavior of this simplified stiffened panel, for example, in images ③ to ⑤ in the graph (Figure 7). The shape of elastic deformations starts from the beginning as the load increases. At 12 ms, the stiffener tripping occurs from the edges, followed by the stiffener center area. This tripping phenomenon indicates that the structure has entered the plasticity regime while the oscillatory response continues to completion.

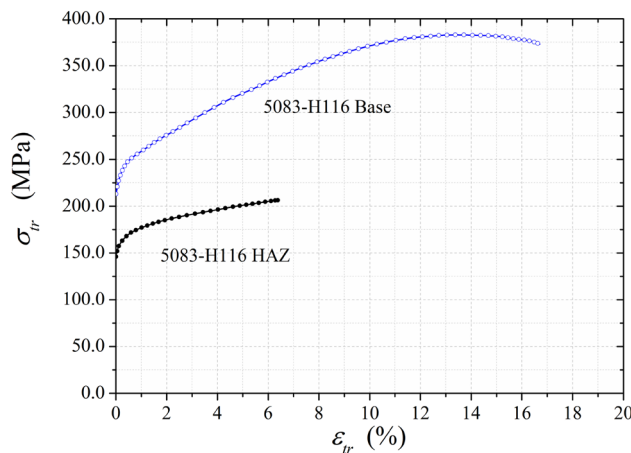
**Figure 5:** True stress–strain test results of 5083-H116 aluminum alloy for the base and HAZ treatment.

Table 2: Validation of FE analysis against benchmark study

Model [Ref]	Material	Pulse duration (ms)	Load (kPa)	Permanent set (mm)		Num/Bench.
				Benchmark	Num	
Model 1a [5]	AL5083-H116	20.00	200	20.00	20.19	1.01
Model 1b [5]	AL5083-H116	20.00	400	60.90	59.20	0.97
Model 2* [11]	AL5083-O	10.27	121	2.51	2.25	0.90
Model 3a** [13]	AL1	$\tau_r = 30, \tau_d = 55$	85	12.00	12.48	1.04
Model 3b*** [13]	AL2	$\tau_r = 28, \tau_d = 67$	100	10.50	7.75	0.74

Original the designated model name: * Model no.1, ** ADR051-1, *** ALD052-2.

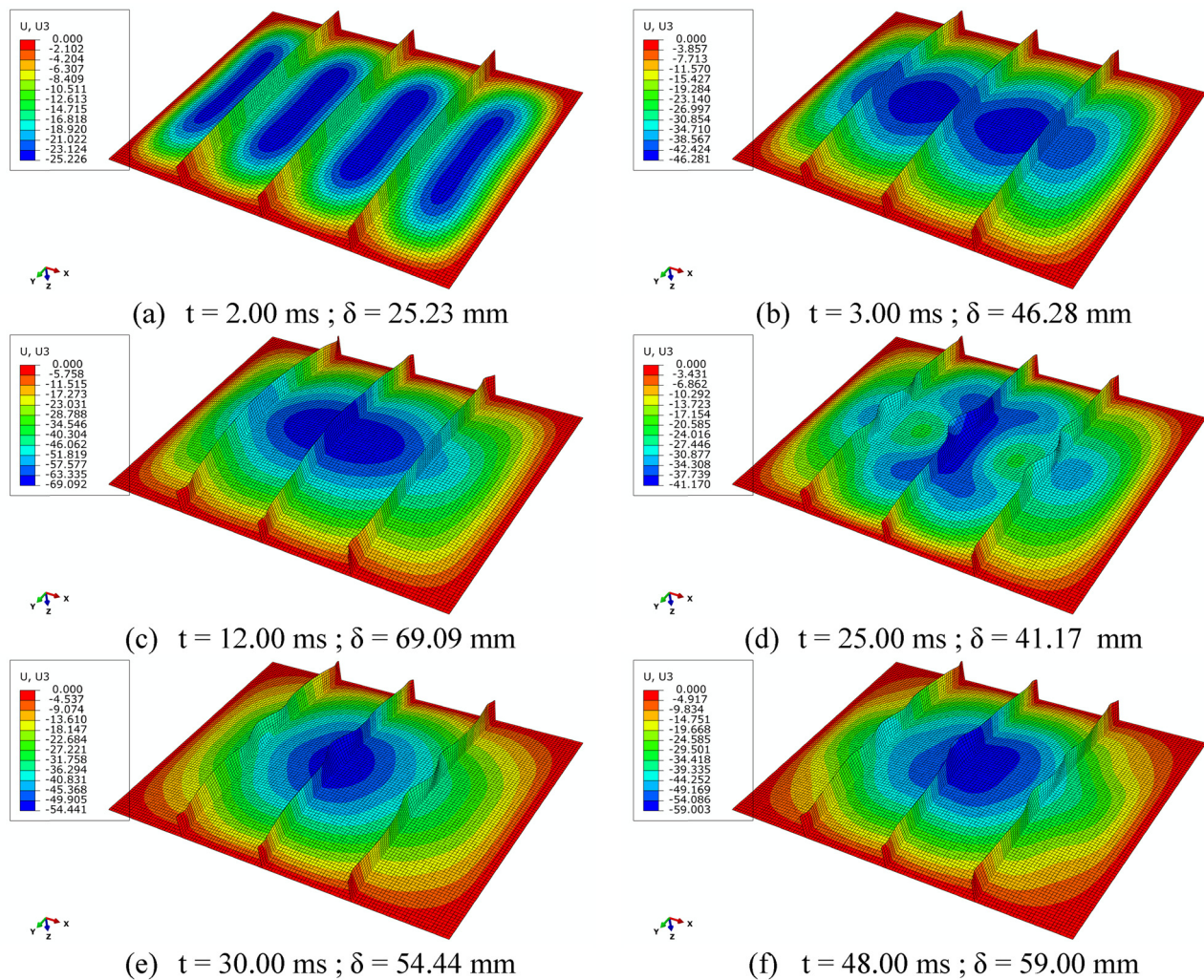


Figure 6: Deformation profile of idealized 80 m high-speed craft bottom panel (model 1b). (a) $t = 2.00$ ms; $\delta = 25.23$ mm. (b) $t = 3.00$ ms; $\delta = 46.28$ mm. (c) $t = 12.00$ ms; $\delta = 69.09$ mm. (d) $t = 25.00$ ms; $\delta = 41.17$ mm. (e) $t = 30.00$ ms; $\delta = 54.44$ mm. (f) $t = 48.00$ ms; $\delta = 59.00$ mm.

The displacement time histories for the model ALD052-2 are plotted in Figure 8. In the simulation, the fixed model represents the fully restrained area of 80 mm on the side area and the bolt constrained, whereas the clamped considering the bolt constrained only. However, the numerical

prediction of the permanent set was under-predicted by around 25%. The edges of the aluminum panels used in the test setup may be more flexible than the pinched conditions used in the numerical model, resulting in discrepancies between numerical and experimental results. In the

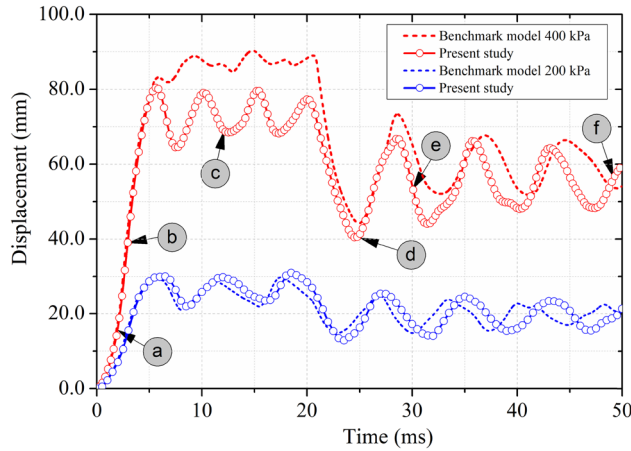


Figure 7: Validation results: Displacement time histories of model 1b.

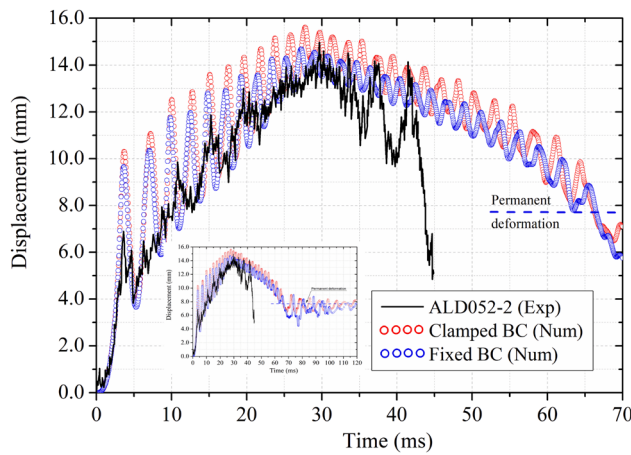


Figure 8: Validation results: Displacement time histories of model 3b.

Table 3: Details of the 30 m class of Indonesian Patrol Vessels

No.	Parameter	Value	Unit
1.	Length overall (L_{oa})	32.00	m
2.	Length of water line (L_{wl})	27.46	m
3.	Breadth (B)	5.85	m
4.	Depth (H)	3.00	m
5.	Draught	1.15	m
6.	High of double bottom	0.90	m
7.	Speed max	28	kN
8.	Material	AL5083-H116, AL6061-T6	

test, the residual plate vibration was not seen in the experimental results because some LVDT sensor settings were broken and could not persist in a set of displacement–time history. The measurements are broken at 43 ms, and the

measured plastic deformations are 10.5 mm. In the maximum elastic deformation, the numerical and test agreed as the value was around 14.0 mm.

3 FE Model of high-speed craft

This numerical simulation aims to obtain the structural responses of the fabricated structures from the 30 m class of Indonesian Patrol Vessels. Table 3 shows the detail of the as-built dimension and materials from the vessel. The vessels were built in a local Indonesian shipyard in Palindo Marine in Batam. The structural layout combination of aluminum stiffened panels that transfer loads to a set of primary transverse frames or girders is described in Figure 9.

3.1 Design criteria

According to the HSC rules [2,3], the design load criteria must be carefully observed in the scantling design of high-speed vessels. The structural design transfers the slamming loads from the bottom plate to longitudinal stiffeners, transverse frames, and primary girders. The details of the slamming design load on the bottom hull according to the HSC rules are as follows:

$$a_{CG} = C_{HSC} \cdot C_{RW} \cdot \frac{V}{\sqrt{L}}, \quad (3)$$

$$V_{FR} = \frac{V}{L^{0.5}}. \quad (4)$$

The first step is calculating the slamming area following the design coefficient of acceleration at the ship's center of gravity (a_{CG}) and the ship's service speed (V_{FR}). Here, C_{HSC} is the service vessel parameter taken as 0.24 for the passenger craft, whereas the service range coefficient (C_{RW}) is taken as 0.9 for restricted ocean service, V is the service speed, and L is the length of the water line.

Then, the slamming load parameter should be calculated as follows:

$$P_{sl} = 100 \cdot T \cdot K_1 \cdot K_2 \cdot K_3 \cdot a_{CG} [\text{kPa}], \quad (5)$$

$$K_3 = \frac{70 - \alpha_d}{70 - \alpha_{dCG}}. \quad (6)$$

Using this design applied load, the structural scantling of the bottom panel can be estimated. Here, T is the



Figure 9: Structural layouts for 30 m class patrol vessels from The Maritime Affairs and Fisheries Ministry of Indonesia.

Table 4: Slamming load calculation according to HSC rules [2,3]

No.	Parameter	Value	Unit
1.	a_{CG}	2.98	g
2.	V_{Fr}	2.55	—
3.	P_{sl}	129	kPa

draught of the craft (m), K_1 is the longitudinal bottom impact pressure distribution factor, starting from 0.5 to 1.0 depending on the distance from the aft perpendicular to the load point. K_2 is the factor accounting for the impact

slamming area for plating, stiffeners, and the girder or floors, which should be taken as a minimum of 0.5, 0.45, and 0.35, respectively. K_3 is the factor accounting for the shape and deadrise of the hull. Value has taken for α_d and α_{dCG} , which are to be between 10 and 30°. The slamming load is calculated based on the above design criteria to evaluate the bottom panel FE structure model. The results are presented in Table 4. It should be noted that the slamming load calculation results from the design rules can be interpreted as design pressure load according to the ship's characteristics. Thus, the parametric studies with a range of up to 250 kPa aim to analyze the behavior up to the

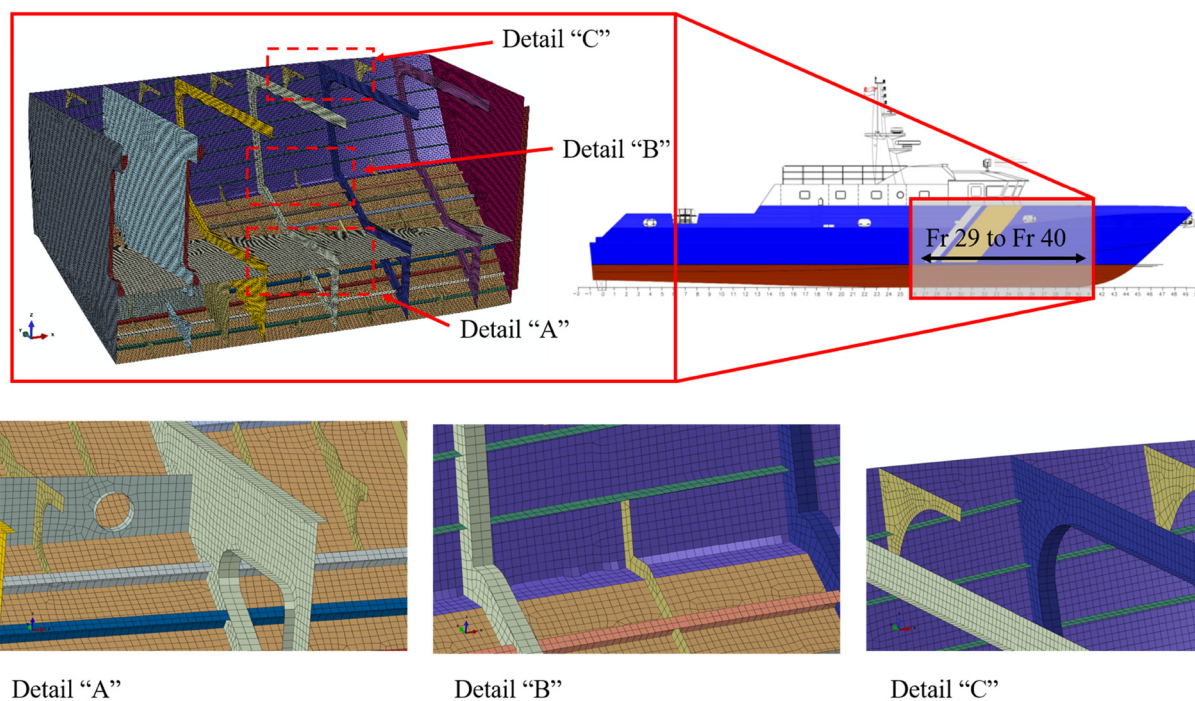


Figure 10: FE model of 30 m class patrol vessels.

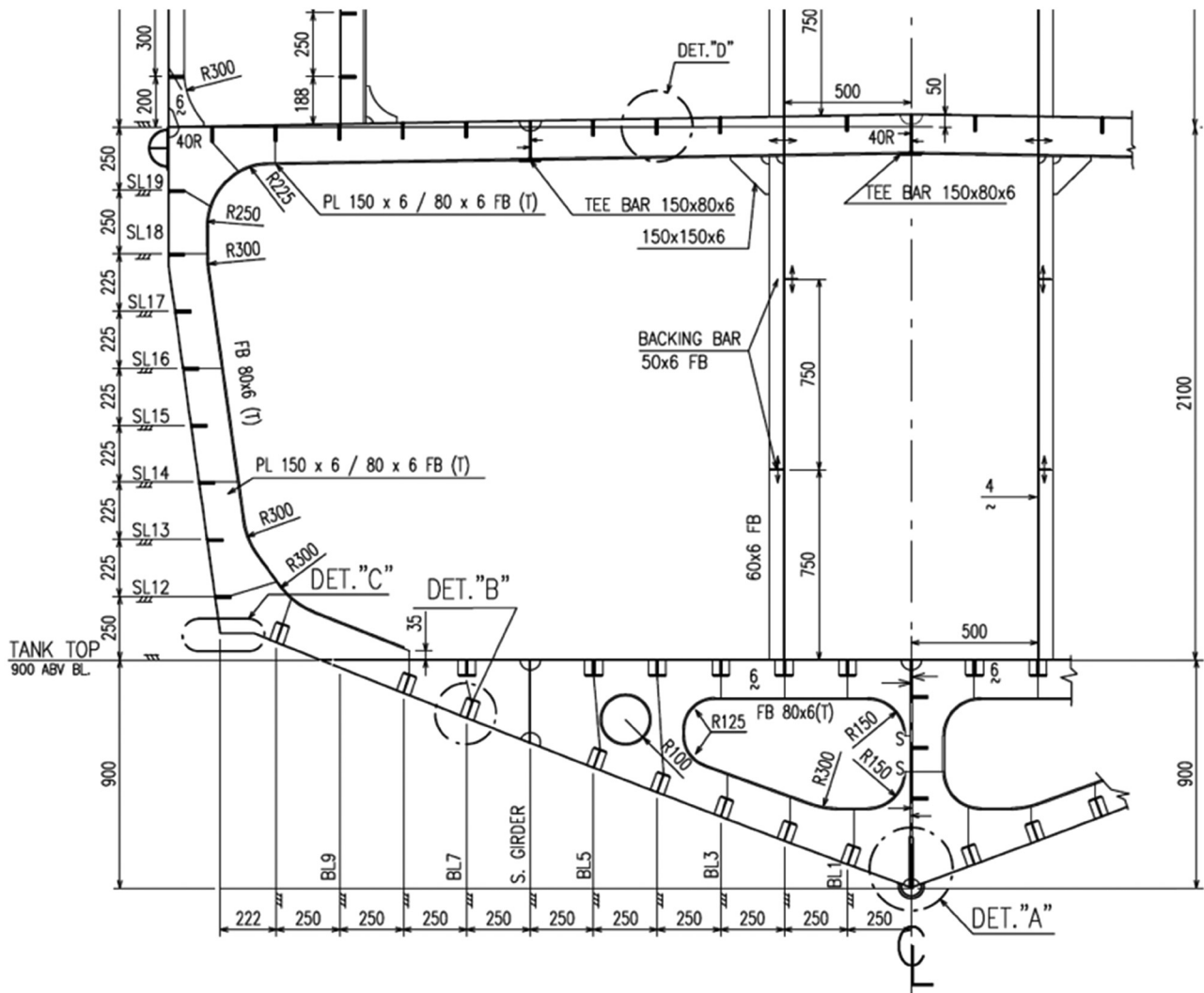


Figure 11: Structural elements in the mid-ship area of 30 m class patrol vessels.

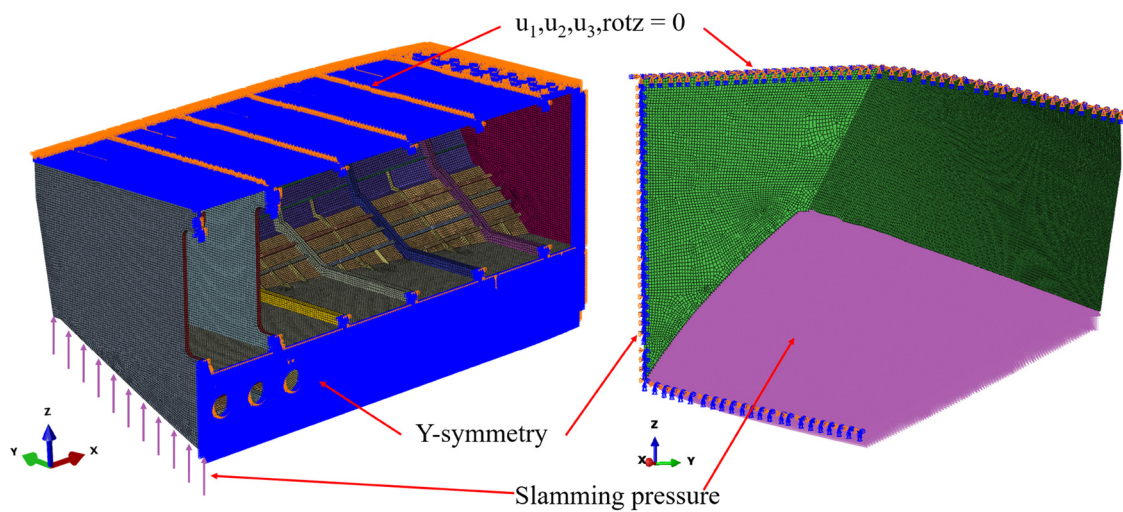


Figure 12: Load and boundary condition of target structures.

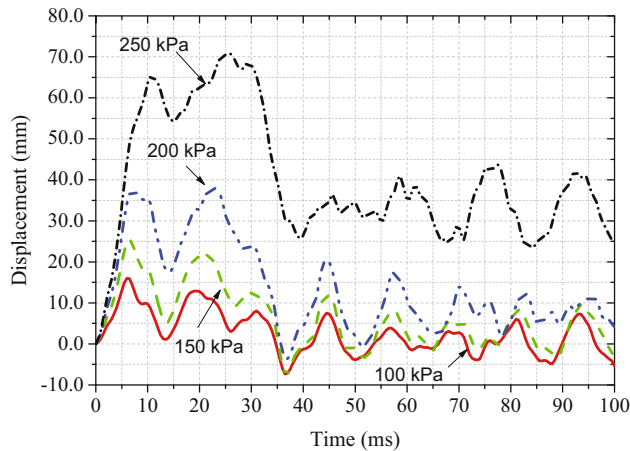


Figure 13: Displacement–time histories at P2 node with increasing pressure from 100 to 250 kPa.

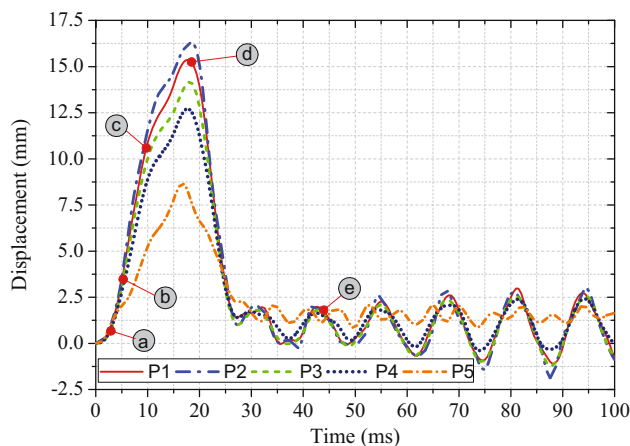


Figure 14: Displacement–time histories of 200 kPa at five different locations.

design limits. The analysis was set at 100 ms to capture the oscillatory behavior after the elastic spring.

3.2 Actual size FE model

The finite element model was created to evaluate structural strength under various loading circumstances. The FE model comprises a limited length of the forward section of frames 29–40. The total length of the FE model was 6,600 mm, whereas the frame spacing was 1,200 mm. The FE model, which includes its subdivision such as frame, shell longitudinal, tanktop plate, deck longitudinal, bottom longitudinal, center, and side girder, are presented in Figure 10.

The FE model is generated using S4R-type shell elements. The shell element is composed of four-node, quad

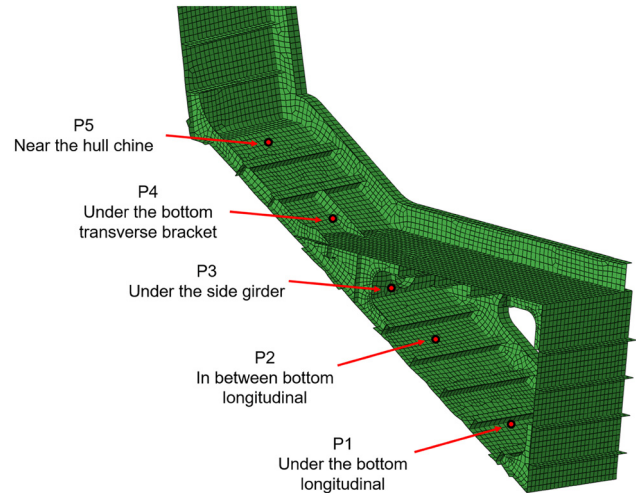


Figure 15: Five displacement trackers were built between web frames 33 and 35.

literal-dominated with reduced integration. The shell element size is approximately 30 mm, which is five times the plate thickness. Considering the size of the structure model, this mesh density is fine enough to capture the deformation. The FE model consists of 135072 shell elements. Figure 11 shows the cross-sectional view of the mid-ship section of a 30 m high-speed craft, which consists of a 6 mm thick plate made of AL5083-H116 and AL6061-T6 [15] for the structural profile.

The same assumption as the methods mentioned earlier for the benchmark models was used in the slamming analysis of this references high-speed craft model. The analyses were run using the explicit solver of the Abaqus software. Figure 12 shows the detail of the load and boundary condition of the half-symmetry FE model. The pressure is applied to the bottom hull up to the chine line with two pressure profile assumptions; rectangular and triangular. At the center edges, the y -axis symmetry was applied. While on the main deck, all degrees of freedom were constrained except for rotation about the x and y -axes.

4 Results and discussion

The complete set of displacement time history measured at P2 node is shown in Figure 13, assuming a rectangular-type slamming load. The response characteristics are clearly visible as the slamming load increases from 100 to 250 kPa. Following the specified design limit (Eq. (5)), the structure is designed for slamming events with 100–150 kPa. Thus, it can be seen that the permanent set increases significantly at a load of 200–250 kPa. The peak load occurs

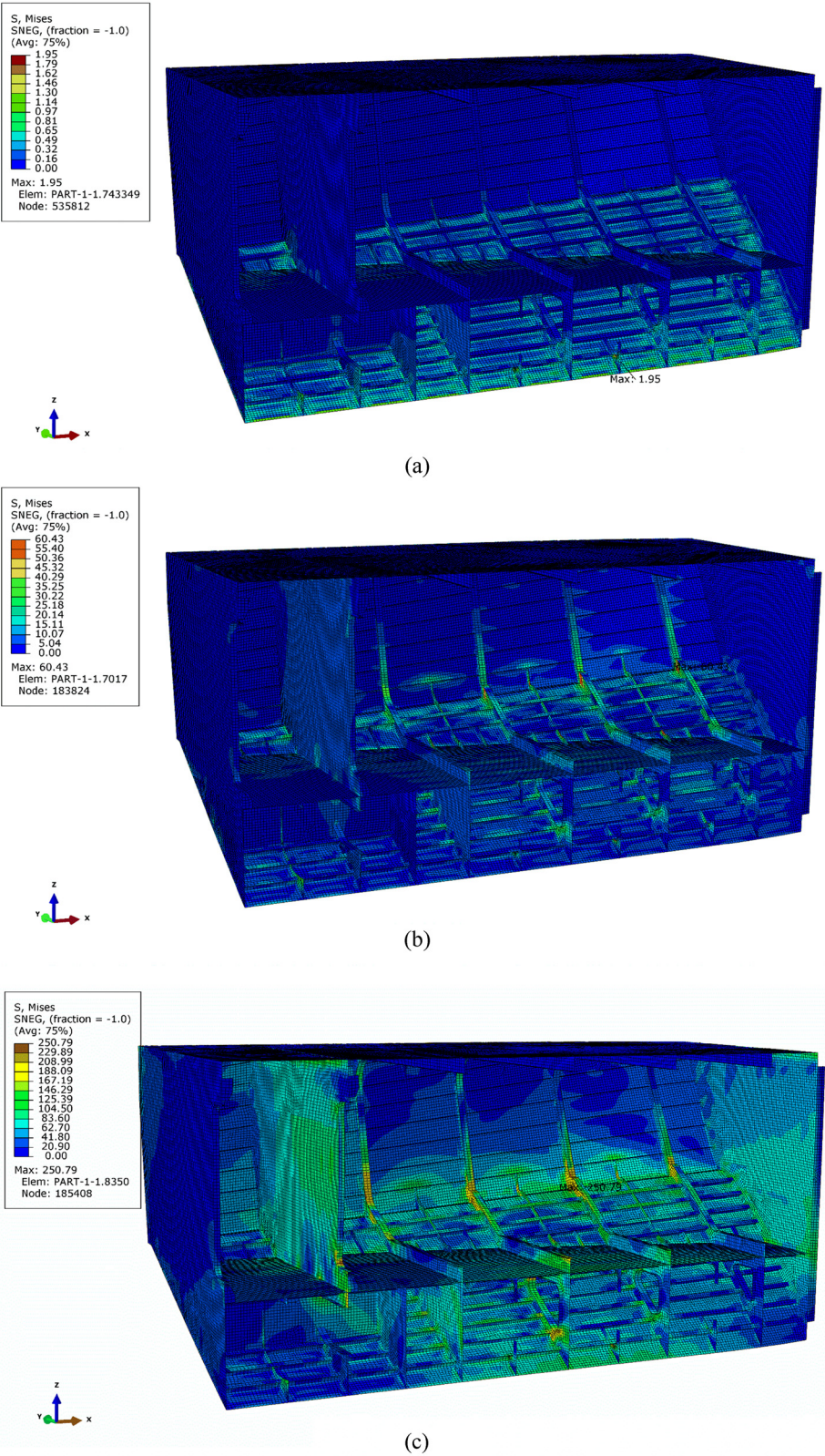


Figure 16: Results from the numerical investigation of the 200 kPa.

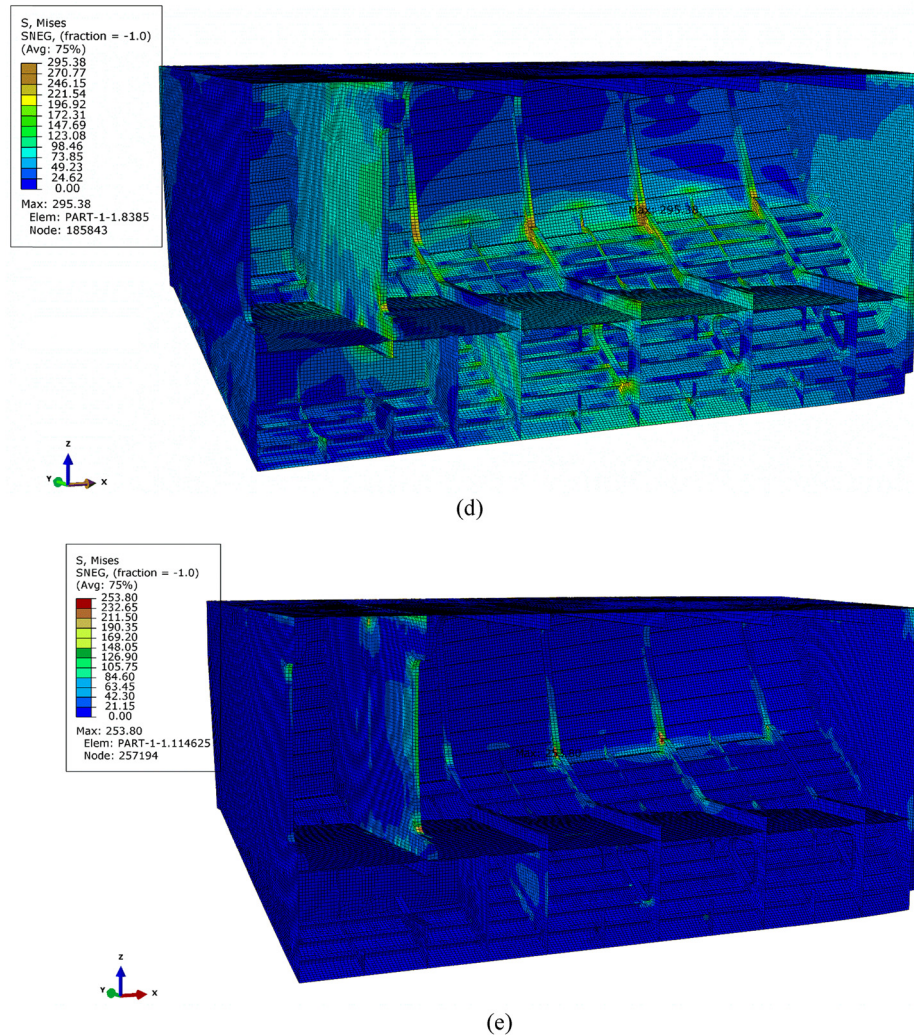


Figure 16: (Continued)

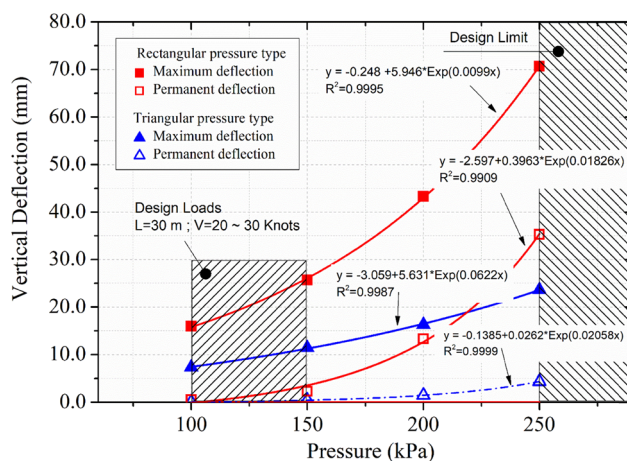


Figure 17: Damage extent of 30 m high-speed craft under two different pressure types.

twice in accordance with the continuous rectangular pressure characteristics.

Figure 14 describes the deformation response according to the slamming time histories for triangular loads. The deformation values were tracked at five different tracer points. From the five monitoring points described in Figure 15, the maximum value of elastic deformation is more significant in the hull bottom plate. The deflection response increases in the plate between the bottom longitudinals. It appears that the girder and longitudinal bottom provides full constraints on the flexibility of the bottom panel structure. From these results, what is interesting is that although the chine area shows the smallest maximum elastic response to deflection, the plastic deformation value is the largest among the five observed areas.

Figure 16 shows the stress fringe plot from a continuous displacement history from the previous figure (Figure 14).

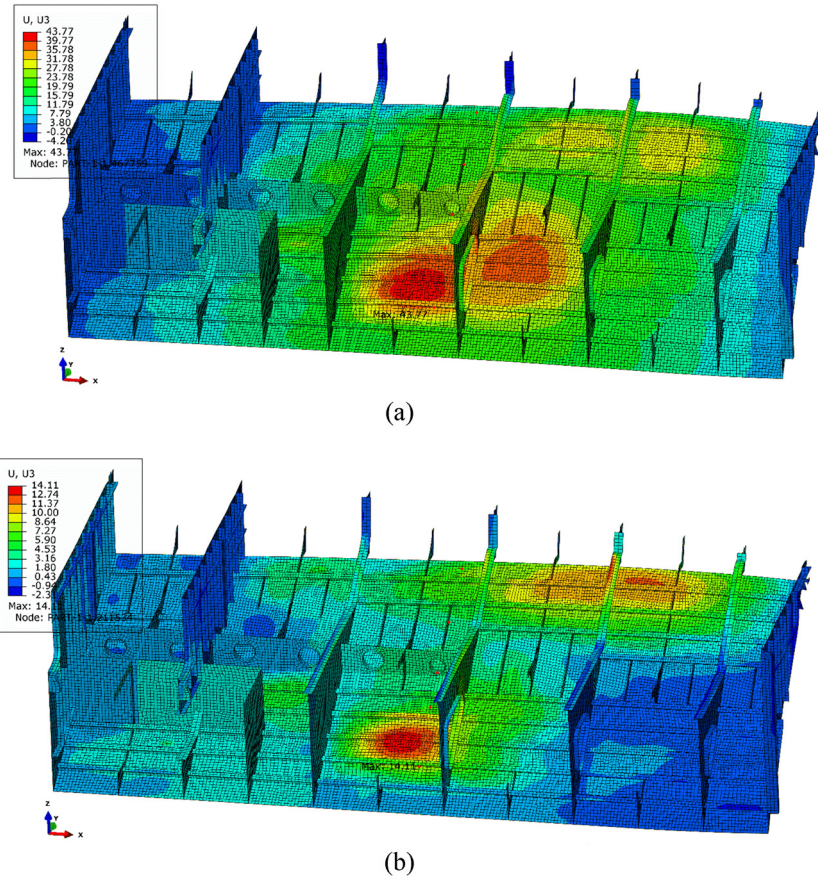


Figure 18: Snapshots of the deformation response within (a) 20 ms and (b) 80 ms for 200 kPa rectangular-type pressure.

The picture with the sequential history shows the effect of triangular pressure loads on the bottom structure of the ship. Following the idealized pressure, the maximum load occurs in the middle of the slamming load's duration, followed by an oscillatory response from the structure after the triangular peak load occurs. At the beginning of the loading, the distribution of the slamming load is continued and divided over an area of the segment between the base plate and the bottom longitudinal, as shown in Figure 16(a). The slamming load is distributed to the web frame structure as the pressure rises. It can be seen that the stress concentration is on the web frame in the chine area, as shown in Figure 16(d). The response of this force distribution is expanding toward the vertical bulkheads, as shown in Figure 16(c) and (d). After passing the peak load, the structure experienced an elastic spring-back. Subsequently, the residual vibrations occurred. The most significant plastic deformation occurred near the chine web frame area, as shown in Figure 16(e).

Lastly, a summary of the pressure to the deformation response is shown in Figure 17. These data show that the rectangular pressure pulse looks more conservative than

the triangular-type pressure. A snapshot of the bottom structure at 200 kPa in Figure 18 shows that the maximum displacement occurs at the center of the FE model in the region between the web frames. The result of permanent plastic deflection increases significantly with the assumed slamming pressure beyond the design loads. This proves that the effective structure is designed below 150 kPa. Although from this analysis, the pressure is modeled up to 250 to describe the limits of the structure's capabilities. The exponential graph of the permanent deflection response between rectangular and triangular pressure shows a difference of up to 85%.

5 Conclusions

This study conducts a comprehensive review of numerical analysis to study the structural behavior under slamming loading. A benchmark analysis taken from the previous study is presented considering the influence of the HAZ on the base material. The primary design calculation

method for slamming load for high-speed craft under the design classification society has also been shown.

In the present analysis, structure deflection varies linearly with a specific pressure range and duration. However, the response of the bottom plate is considerably affected by the type of the idealized pressure profile (rectangular and triangular). The results of the rectangular-type pressure showed that it was more severe than the triangular. As a result, while evaluating the structural integrity of this high-speed craft, it is important to properly take into account the realistic pressure-time history from slamming.

The analysis shows a tendency for stress concentration in the web frame in the chine area. Thus, it can be recommended for a typical hull model. In addition, a bracket support structure is needed to distribute the web frame load in this area.

The slamming load calculated using the design rules from the BKI shows a good agreement with the simulation results. It is clear that using a slamming load over the design load considerably increases the permanent set response.

Further investigation seems necessary regarding the effects of the strain rate hardening and the ductile damage constitutive material on the dynamic response of marine aluminum-alloy plates to impulsive pressure loadings. In addition, more testing on the material is required to support the analysis of mechanical properties with the HAZ treated.

Acknowledgments: This work is part of the research activity “Crashworthiness Analysis in a Fishery Patrol Vessel Collision as an Accident Mitigation During an Ambush Mission” conducted by the Marine Numerical Safety Analysis research group collaborated with Floating Structures Shipping System Technology research group under the support from Research Organization for Energy and Manufacture, National Research and Innovation Agency (BRIN) research grant DIPA No. 124.01.KB.6693.SDB.001.051.A.

Funding information: National Research and Innovation Agency (BRIN), research grant DIPA No. 124.01.KB.6693.SDB.001.051.A.

Author contributions: All authors have accepted responsibility for the entire content of this manuscript and approved its submission. Muryadin: methodology and mentorship to the core team in the previous work, writing – review and editing. Teguh Muttaqie: principal investigator, conceptualization, validation, writing – original draft, writing – review and editing. Cahyo Sasmito: methodology, provision of test materials and computing resources,

writing – review and editing. Fariz Maulana N: methodology, writing – review and editing. Andi C.P.T. Nugroho: methodology, investigation. Dany Hendrik P.: methodology, formal analysis. Buddin Al Hakim: methodology, project administration. Abid Paripurna F.: methodology, visualization. Muh Hisyam K.: methodology, visualization. Teguh Wibowo: management and coordination responsibility for the previous research. Arfis Maydino F.P.: methodology and visualization.

Conflict of interest: The authors state no conflict of interest.

Data availability statement: The authors declare that the data supporting the findings of this study are available within the article.

References

- [1] Kapsenberg GK. Impulsive pressure loading and response assessment. In: Jang CD and Hong SY, editors. Proceedings of the 17th International Ship and Offshore Structures Congress, ISSC'09; 2009 Aug 16–21; Seoul, Korea. Seoul National University, 2009. ISBN: 978-89-954730-1-6.
- [2] Biro Klasifikasi Indonesia. Rules for High Speed Craft. Volume III, Part 3. Special Ships. Jakarta, Indonesia: Biro Klasifikasi Indonesia; 2022.
- [3] Biro Klasifikasi Indonesia. Rules for Hull. Volume II. Part 1. Seagoing Ships. Jakarta, Indonesia: Biro Klasifikasi Indonesia; 2022.
- [4] Razola M. New perspectives on analysis and design of high-speed craft with respect to slamming [dissertation]. Stockholm: Kungliga Tekniska Högskolan; 2016.
- [5] Liu B, Villavicencio R, Liu K, Zhu L, Guedes Soares C. Response of an aluminum stiffened plate under extreme slamming loadings. *J Offshore Mech Arct Eng*. 2019 Oct 1;141(5):051606.
- [6] Cerik BC. Large inelastic deformation of aluminium alloy plates in high-speed vessels subjected to slamming. *J Mar Sci Technol*. 2017 Jun;22:301–12.
- [7] Cerik BC. Damage assessment of marine grade aluminium alloy-plated structures due to air blast and explosive loads. *Thin-Walled Struct*. 2017 Jan 1;110:123–32.
- [8] Seo B, Truong DD, Cho S, Kim D, Park S, Shin H. A study on accumulated damage of steel wedges with dead-rise 10 due to slamming loads. *Int J Nav Archit Ocean Eng*. 2018 Jul 1;10(4):520–8.
- [9] Truong DD, Shin HK, Cho SR. Permanent set evolution of aluminium-alloy plates due to repeated impulsive pressure loadings induced by slamming. *J Mar Sci Technol*. 2018 Sep;23:580–95.
- [10] Paik JK, Duran A. Ultimate strength of aluminum plates and stiffened panels for marine applications. *Mar Technol SNAME N*. 2004 Jul 1;41(3):108–21.

- [11] Mori K. Response of the bottom plate of high speed crafts under impulsive water pressure. *J Soc Nav Archit Jpn.* 1977;1977(142):297–305. (in Japanese)
- [12] Truong DD, Jang BS, Janson CE, Ringsberg JW, Yamada Y, Takamoto K, et al. Benchmark study on slamming response of flat-stiffened plates considering fluid-structure interaction. *Mar Struct.* 2021 Sep 1;79:103040.
- [13] Langdon GS, Schleyer GK. Inelastic deformation and failure of clamped aluminium plates under pulse pressure loading. *Int J Impact Eng.* 2003 Nov 1;28(10):1107–27.
- [14] Muttaqie T, Park SH, Sohn JM, Cho SR, Nho IS, Han S, et al. Implosion tests of aluminium-alloy ring-stiffened cylinders subjected to external hydrostatic pressure. *Mar Struct.* 2021 Jul 1;78:102980.
- [15] Simulia DS. Abaqus analysis user's manual. Version 6.23. Dassault Systemes. Pawtucket, USA; 2021.